Assessment of alveolar bone marrow fat content using 15 T MRI

Arthur Rodriguez Gonzalez Cortes, DDS, PhD,[a,b,c] Ouri Cohen, PhD,[a,b] Ming Zhao, PhD,[a,b,d]
Eduardo Massaharu Aoki, DDS, PhD,[c] Rodrigo Alves Ribeiro, DDS, PhD,[e] Lina Abu Nada, DDS, MS,[f]
Claudio Costa, DDS, PhD,[c] Emiko Saito Arita, DDS, PhD,[c] Faleh Tamimi, DDS, PhD,[f] and
Jerome L. Ackerman, PhD[a,b]

Objectives. Bone marrow fat is inversely correlated with bone mineral density. The aim of this study is to present a method to quantify alveolar bone marrow fat content using a 15 T magnetic resonance imaging (MRI) scanner.

Study Design. A 15 T MRI scanner with a 13-mm inner diameter loop-gap radiofrequency coil was used to scan seven 3-mm diameter alveolar bone biopsy specimens. A 3-D gradient-echo relaxation time (T1)–weighted pulse sequence was chosen to obtain images. All images were obtained with a voxel size (58 μm^3) sufficient to resolve trabecular spaces. Automated volume of the bone marrow fat content and derived bone volume fraction (BV/TV) were calculated. Results were compared with actual BV/TV obtained from micro-computed tomography (CT) scans.

Results. Mean fat tissue volume was 20.1 ± 11%. There was a significantly strong inverse correlation between fat tissue volume and BV/TV (r = –0.68; *P* = .045). Furthermore, there was a strong agreement between BV/TV derived from MRI and obtained with micro-CT (interclass correlation coefficient = 0.92; *P* = .001).

Conclusions. Bone marrow fat of small alveolar bone biopsy specimens can be quantified with sufficient spatial resolution using an ultra-high-field MRI scanner and a T1-weighted pulse sequence. (Oral Surg Oral Med Oral Pathol Oral Radiol 2018;125:244–249)

Morphologic conditions of the alveolar bone may have an impact on outcomes of different dental treatment modalities, such as implant dentistry and periodontology.[1,2] Alveolar bone density has been quantified in vivo with computed tomography (CT) methods[1,3] and ex vivo with histomorphometry[4] and micro-CT.[3] Alveolar bone density also plays an important role in dental implant osseointegration, where an inverse relationship has been determined between the contact extension between implant body and bone marrow fat.[5] Bone mineral density and bone volume fraction (defined as bone volume over total volume; BV/TV) generally vary inversely with yellow bone marrow fat (BMF) content,[6] which may therefore also have an impact on dental treatments. Furthermore, BMF quantification is also important in radiotherapy to prevent and detect marrow composition changes that could lead to hematologic toxicity.[7,8]

BMF is commonly measured with magnetic resonance imaging (MRI).[9] In MRI, images are formed from radiofrequency signals that are generated from the spins of the nuclei (^{1}H) of hydrogen atoms. In bones, hydrogen atoms can be found mainly in the water and protein in the bone matrix and in the water and fat in bone marrow. However, trabecular bone measurements with MRI at conventional magnetic field strengths are challenging because of limited signal-to-noise ratio (SNR) resulting in low spatial resolution that is often insufficient to visualize individual marrow spaces.[10] Therefore, to obtain adequate SNR from small bone specimens, the use of small high-performance radiofrequency (RF) coils as well as high magnetic fields is required. Little is known of the benefits of using an ultra-high-field (15 T) MRI scanner with custom-built RF coils to analyze the small (3 mm diameter) bone specimens commonly used in studies on alveolar bone and dental implants.[1]

Statement of Clinical Relevance

This is the first study on magnetic resonance imaging for alveolar bone morphometry. According to the evidence discussed here, with sufficient development our methodology may be adapted to clinical magnetic resonance imaging scanners. This would allow for assessing conditions of alveolar bone in patients without the need of ionizing radiation.

A postdoctoral scholarship was granted to ARGC by the National Council for Scientific and Technological Development (CNPq), Science without Borders, Brazil (no. 232643/2013-0). Another research scholarship was also granted to ARGC by Lemann Foundation (CsF/Lemann Scholarship – 03-2015, Brazil). This research was also supported in part by the Athinoula A. Martinos Center for Biomedical Imaging and the Center for Functional Neuroimaging Technologies (funded by NIH grant P41-EB015896). The 15 T scanner was developed with High End Instrumentation Grant S10 RR023009 from the National Center for Research Resources of the National Institutes of Health. F.T. was supported by Canada Research Chair.

[a]Martinos Center for Biomedical Imaging, Department of Radiology, Massachusetts General Hospital, Charlestown, Massachusetts, USA.
[b]Department of Radiology, Harvard Medical School, Boston, Massachusetts, USA.
[c]Department of Oral Radiology, School of Dentistry, University of São Paulo, São Paulo, Brazil.
[d]Department of Physics, University of Massachusetts Lowell, Lowell, Massachusetts, USA.
[e]Department of Oral Implantology, School of Dentistry, Metropolitan University of Santos, Santos, Brazil.
[f]Faculty of Dentistry, McGill University, Montreal, Quebec, Canada.

Received for publication Jun 15, 2017; returned for revision Nov 3, 2017; accepted for publication Nov 11, 2017.

2212-4403/$ - see front matter
https://doi.org/10.1016/j.oooo.2017.11.016

Thus, the aim of this study was to present a method to assess and quantify the BMF content from small alveolar bone samples using a 15 T MRI scanner with a custom-built RF coil.

MATERIALS AND METHODS

Patients

This study was approved by the ethics committee of the University of São Paulo (protocol number: 104/11). An informed consent form was signed by all patients willing to participate in this study. The guidelines of the Helsinki Declaration were followed in this investigation.

Inclusion and exclusion criteria

This study was conducted on cylindrical bone samples from partially edentulous patients attending a private dental clinic that has a research partnership with the University of São Paulo, Brazil. One bone specimen per patient was assessed. All patients had been referred for implant placement (maximum of 1 implant per dental arch, regardless of the number of missing teeth) between October 2014 and March 2015. Only mandibular implant sites more than 5 mm in width were included.

Patients with metabolic disorders, such as vitamin D deficiency and diabetes or those with insufficient alveolar bone volume for implant placement were excluded from the study. History of ridge grafting was also considered an exclusion criterion.

Bone sample preparation

All bone specimens had been retrieved at time of implant placement by using a trephine burr (3 mm internal diameter) to prepare the implant sites. In all cases, implants were successfully placed, restored, and followed up for a minimum of 1 year. No postoperative complications were observed during this period.

All specimens had the same dimensions (3 mm diameter and 6 mm length) and were fixed in 10% buffered formalin, in accordance with previously described methodologies for trabecular bone assessement.[11,12] Before the scans, the surfaces of all specimens were patted dry to minimize contamination of the total proton signal by the formalin proton signal. The specimens were then transferred to 13-mm glass nuclear magnetic resonance tubes containing liquid fluorocarbon (Fomblin perfluoropolyether, Ausimont, Thorofare, NJ). This fluid does not contain hydrogen atoms and eliminates the intense proton signal from the fixation medium, mitigates susceptibility difference artifacts at tissue–air interfaces, and slows sample dehydration.

RF coil

A custom-built RF probe based on a loop–gap–resonator design,[13] with a 13-mm inner diameter (ID) (Figure 1) was used for all measurements at room temperature. To build the RF coil, coaxial cylinders made of plastic (outer cylinder) and quartz (inner cylinder) were used as formers for the coupled resonators. Both cylinders were covered with self-adhesive copper tape (Scotch Brand Foil Tapes, 3 M, Inc., Minneapolis, MN) split into 2 parts by 5- and 2-mm gaps for the outer and inner cylinders, respectively. The gap widths were chosen to adjust the resonance frequency of the resonator to that of the 619 MHz Larmor frequency of the scanner. Adhesive Teflon tape was used to secure the copper tape to allow smooth rotation of the 2 cylinders and increase the dielectric constant of the intercylinder space. The gap in the inner cylinder was bridged by a 24 mm long × 8 mm wide copper tape patch to improve the RF magnetic field homogeneity.

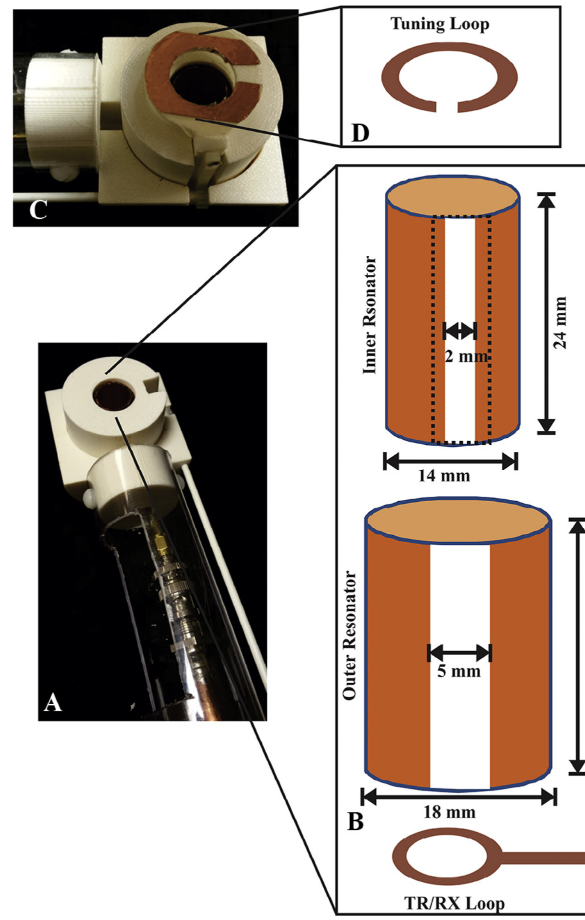

Fig. 1. Photographs of the radiofrequency (RF) coil design **(A)**, along with exploded view illustrations **(C–D)**. Relative rotation of the concentric resonators provides tuning of the coil frequency. An additional piece of copper foil *(dotted rectangle)*, insulated from both cylinders and rotating with the inner cylinder, was used to bridge the gap on the inner resonator and improve the RF homogeneity. Adjusting the height of the loop above the coil with the gear and rack mechanism **(C)** allowed fine-tuning of the resonance frequency of the coil while inside the scanner. Coupling to the scanner was achieved using the transmit/receive (TR/RX) loop shown.

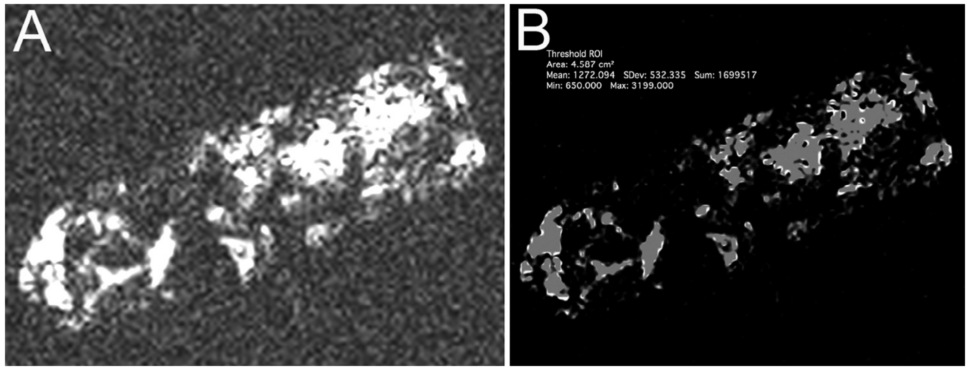

Fig. 2. Automated segmentation of the bone marrow fat content in a small (3 mm in diameter) bone specimen. **A,** Original T1-weighted longitudinal image of a single slice. **B,** Automated segmentation of the bone marrow fat (BMF) area of the same slice.

MRI scans

All scans were performed on a 15 T 130-mm horizontal bore magnet (Agilent, Yarnton, Oxford, UK) equipped with a 60-mm ID gradient insert (Resonance Research, Inc., Billerica, MA) with 2370 mT/m maximum gradient, interfaced to a Siemens console (Siemens Medical Systems, Erlangen, Germany). Before the imaging procedure, the presence of a weak water signal peak (observed at a chemical shift of 4.7 ppm), presumed to be predominantly from residual formalin, and a strong fat signal peak (at 1.3 ppm) was confirmed in all cases by means of a spectroscopy assessment that is normally performed by the 15 T scanner during its frequency tuning procedure. This confirmed that the signal from these specimens was predominantly from marrow fat. All scans were acquired with a field of view of $7.5 \times 7.5 \times 7.5$ mm and a matrix of $128 \times 128 \times 128$ pixels, yielding voxel dimensions of 59 μm^3 (0.20 pL).

RF pulse sequence to detect fat tissue

A 3-D gradient-echo pulse sequence was used in all scans with a 255-Hz receiver bandwidth, 25-degree flip angle, 16 averages, 50 ms repetition time (TR) and 3.3 ms echo time (TE), resulting in a total acquisition time of 32:07 min:s per scan.

Fat protons occur overwhelmingly in the methylene groups in the hydrophobic chains of lipid molecules, and generally exhibit a much shorter spin-lattice relaxation time (T1) compared with water molecules in pure water or in marrow. Because the T1 of the water in formalin is similar to that of pure water, the short TR used in the pulse sequence tends to suppress signals from water in residual formalin as well as from erythropoietic (red) marrow, while retaining the signals from fatty (yellow) marrow.[9,14,15]

BMF content measurement

All analyses were performed on Digital Imaging and Communications in Medicine (DICOM) files using an open-source DICOM viewer (OsiriX v. 6.0; Pixmeo, Geneva, Switzerland). A region of interest (ROI) enclosing the total estimated volume with fat tissue was generated using a previously described methodology.[14] The threshold was defined according to the histogram of the signal intensities (12-bit pixel values). An optimized lower threshold value of 2000 was estimated and set for all measurements. Accordingly, all pixels with a value greater than 2000 were classified as fat tissue and included in the autogenerated ROI (Figure 2). The 3-D ROI measurement tool of the software was then used to calculate the volume of the ROI in cubic millimeters. Because this method for measuring an automated ROI is highly reproducible,[16] a single observer with expertise in radiology (PhD in oral radiology and postdoctoral fellow trained in radiology and nuclear magnetic resonance science) performed all volume calculations.

Derived BV/TV calculation

The MRI scans obtained were also used to calculate BV/TV, as previously described.[10] Briefly, binary images were created with the assumption that dark pixels correspond to bone tissue. For this purpose, water and fat proportions were not taken into consideration because the water content is extremely low, and the main objective was to calculate the percentage of the volume that corresponds to bone tissue.

Micro-CT analysis

A micro-CT scanner (SkyScan1172; SkyScan; Kontich, Belgium) was used to analyze the bone specimens with the source running at 100 kV and 100 μA, a voxel size of 6.0 μm, with a 0.5 mm aluminum filter. Time exposure per frame was 450 ms. The Nrecon (Sky-Scan, Kontich, Belgium) software was used to reconstruct the resulting X-ray images, which were further analyzed for BV/TV. All micro-CT analyses were performed by an examiner with expertise in bone morphometry (PhD student and master in biomaterials).

Statistical analysis

Because strong correlations were expected, the sample size used was determined to detect a minimum correlation of 0.8, to give the study a power of 80% at a significance level of 5%. Normality of all variables was assessed using Shapiro-Wilk's test. Pearson's test was used to assess the correlation between the total fat volume and BV/TV, and agreement between BV/TV from MRI and micro-CT was calculated with the intra-class correlation coefficient. All statistical analyses were performed at a level of significance of 5%, using SPSS version 17 (SPSS, Inc., Chicago, IL).

RESULTS

Seven patients—totaling 7 bone specimens (1 per subject)—were included in this study (Table I). All patients were females (mean age 53.7 ± 4.4 years). Mean fat tissue volume was 20.1% ± 11.3%. There was a significantly strong inverse correlation between fat tissue volume and BV/TV obtained with micro-CT ($r = -0.68$; $P = .045$) (Figure 3). Furthermore, there was also a strong agreement between BV/TV derived from MRI and that obtained with micro-CT (intra-class correlation coefficient = 0.92; $P = .001$).

Table I. Results for BMF measurements of each bone sample

		15 T MRI		Micro-CT
Bone sample	*Patient's age, y*	*Fat tissue volume (%)**	*Derived BV/TV (%)†*	*BV/TV (%)*
1	55	16.30	76.30	66.39
2	51	4.86	96.11	94.60
3	61	39.34	75.14	73.10
4	47	20.55	75.67	78.97
5	56	14.90	86.20	84.68
6	52	30.04	65.18	63.22
7	54	15.39	83.22	85.73

15 T MRI, 15 Tesla magnetic resonance imaging; *BMF,* bone marrow fat; *BV/TV,* bone volume fraction; *micro-CT,* micro-computed tomography.

*Results are significantly inversely correlated with micro-CT BV/TV, according to Pearson's test ($r = -0.684$; $P = .045$).

†Results are in strong agreement with micro-CT BV/TV, according to the intraclass correlation coefficient (0.920; $P = .001$).

DISCUSSION

Bone marrow fat quantification with MRI has been described as a promising diagnostic method despite challenges in obtaining high-resolution images.[11,14,15,17] The present findings indicate that quantification of BMF content in small specimens is feasible using a T1-weighted gradient echo pulse sequence and a custom made RF coil in a 15 T MRI scanner. The high SNR provided by the strong magnetic field and large filling factor of the coil led to high spatial resolution with voxel size of 59 μm^3 and consequently improved image quality. The improved resolution allowed greater contrast between pixels and facilitated the subsequent automated volume measurements (segmentation) of the fat content. The automatic segmentation technique used here has been shown to compute fat tissue volumes accurately on T1-weighted images.[18] In particular, the reproducibility of the measurements was not affected by the choice of segmentation algorithm.

To our knowledge, this is the first application of ultra-high-field MRI in bone morphometry for dental research, supporting the findings of previous medical studies.[9,12,14,15,17,19] BMF quantification has been shown to yield clinically relevant data in the detection of bone marrow alterations associated with radiotherapy.[7,8] In accordance with our findings, clinical applications of T1-weighted images have also been described to detect the increase of BMF volume resulting from radiation therapy.[20-22]

Alveolar bone research frequently involves the use of small-diameter jaw specimens obtained with a trephine. Imaging and structural findings of alveolar bone have been correlated with bone grafts and dental implant outcomes[1,2] and systemic bone findings.[23] As demonstrated in this study, fat content assessment using MRI can be achieved with pulse sequences that emphasize differences in T1 between water and fat.[6,9,14,15]

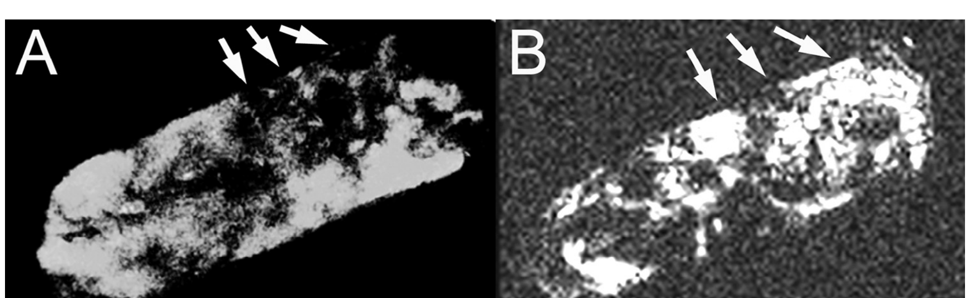

Fig. 3. Correlation between 15 T magnetic resonance imaging (MRI) and micro-computed tomography (micro-CT). **A,** Micro-CT reconstruction of a bone sample, showing areas with absence of bone tissue *(arrows)*. **B,** 15 T MRI of the same bone sample, showing that the areas without bone tissue generally had a large fat content *(arrows)*.

Importantly, the inverse relationship between morphometric BV/TV and BMF enables indirect assessment of actual bone volume fraction. A recent animal study on dental implants suggested that implant osseointegration is enhanced in the presence of blood clots and indirectly proportional to the extension of the contact between the implant body and BMF.[5] Therefore, quantifying the fat content in jaws may indicate sites that are more favorable for dental implant installation. Although the present MRI methodology is indicated for BMF assessment, other MRI protocols could be used for dental implant surgical planning.[24-26] Further clinical studies would be recommended to address possible clinical advantages of incorporating the fat quantification method described in this proof-of-concept study.

This investigation had several limitations. First, because only bone specimens were scanned, and in anticipation of the eventual use of this technique in vivo, the effect of motion artifacts in live human patients could not be ascertained. Nevertheless, similar methodologies have been adapted to clinical scanners to measure BMF in vivo with optimized pulse sequences, and our methodology could be similarly adapted as well.[6,9,14,15] An additional limitation is that only samples from female patients were analyzed. Further studies with larger sample sizes on clinical scanners testing different pulse sequence parameters would be recommended to address the in vivo feasibility of the methodology presented here.

In this study, water and fat content were not unambiguously and quantitatively assessed with spectroscopic measurements, such as quantitative water and fat imaging with the use of Dixon or similar MRI pulse sequences.[27] The use of the chemical shift difference between water and fat in MR spectroscopy or spectroscopic imaging in trabecular bone can be challenging at very high fields because of the significant line broadening caused by the increased magnetic susceptibility effect in trabecular bone.[10] This effect hinders a clean separation of water and fat content, adds to the duration of the measurement, and reduces the SNR when images must be combined by addition or subtraction. In contrast, the use of T1 weighting is a well-established method and relatively quick to perform.[6,9,14,15] Furthermore, because it is generally established that the marrow of the mandible is predominantly yellow, especially in adult patients who are likely to be receiving dental implants,[15] it is reasonable to assume that the MRI signal in the specimens examined in this study comes predominantly from fat, which further supports the clinical relevance of this study.

CONCLUSIONS

In spite of the limitations of this study, our findings suggest that BMF of small alveolar bone samples can be segmented with satisfactory contrast resolution using an ultra-high-field MRI scanner with a customized coil of small diameter and a T1-weighted pulse sequence. To our knowledge, this is the first demonstration of alveolar bone morphometry using MRI to estimate BV/TV, validated by means of micro-CT morphometric analyses.

REFERENCES

1. Cortes AR, Eimar H, Barbosa Jde S, Costa C, Arita ES, Tamimi F. Sensitivity and specificity of radiographic methods for predicting insertion torque of dental implants. *J Periodontol*. 2015;86:646-655.
2. Cortes AR, Pinheiro LR, Cavalcanti MG, Arita ES, Tamimi F. Sinus floor bone failures in maxillary sinus floor augmentation: a case-control study. *Clin Implant Dent Relat Res*. 2015;17:335-342.
3. Parsa A, Ibrahim N, Hassan B, van der Stelt P, Wismeijer D. Bone quality evaluation at dental implant site using multislice CT, micro-CT, and cone beam CT. *Clin Oral Implants Res*. 2015;26:e1-e7.
4. Parfitt AM, Drezner MK, Glorieux FH, et al. Bone histomorphometry: standardization of nomenclature, symbols, and units. Report of the ASBMR Histomorphometry Nomenclature Committee. *J Bone Miner Res*. 1987;2:595-610.
5. Morelli F, Lang NP, Bengazi F, Baffone D, Vila Morales CD, Botticelli D. Influence of bone marrow on osseointegration in long bones: an experimental study in sheep. *Clin Oral Implants Res*. 2015;26:300-306.
6. Schwartz AV. Marrow fat and bone: review of clinical findings. *Front Endocrinol (Lausanne)*. 2015;6:40.
7. Carmona R, Pritz J, Bydder M, et al. Fat composition changes in bone marrow during chemotherapy and radiation therapy. *Int J Radiat Oncol Biol Phys*. 2014;90:155-163.
8. Curi MM, Cardoso CL, de Lima HG, Kowalski LP, Martins MD. Histopathologic and histomorphometric analysis of irradiation injury in bone and the surrounding soft tissues of the jaws. *J Oral Maxillofac Surg*. 2016;74:190-199.
9. Shen W, Chen J, Punyanitya M, Shapses S, Heshka S, Heymsfield SB. MRI-measured bone marrow adipose tissue is inversely related to DXA-measured bone mineral in Caucasian women. *Osteoporos Int*. 2007;18:641-647.
10. Magland JF, Wehrli FW. Trabecular bone structure analysis in the limited spatial resolution regime of in vivo MRI. *Acad Radiol*. 2008;15:1482-1493.
11. Baum T, Kutscher M, Muller D, et al. Cortical and trabecular bone structure analysis at the distal radius-prediction of biomechanical strength by DXA and MRI. *J Bone Miner Metab*. 2013;31:212-221.
12. Wurnig MC, Calcagni M, Kenkel D, et al. Characterization of trabecular bone density with ultra-short echo-time MRI at 1.5, 3.0 and 7.0 T—comparison with micro-computed tomography. *NMR Biomed*. 2014;27:1159-1166.
13. Ono M, Suenaga A, Hirata H. Experimental investigation of RF magnetic field homogeneity in a bridged loop-gap resonator. *Magn Reson Med*. 2002;47:415-419.
14. Vande Berg BC, Malghem J, Lecouvet FE, Maldague B. Magnetic resonance imaging of normal bone marrow. *Eur Radiol*. 1998;8:1327-1334.
15. Yamada M, Matsuzaka T, Uetani M, Hayashi K, Tsuji Y, Nakamura T. Normal age-related conversion of bone marrow in the mandible: MR imaging findings. *AJR Am J Roentgenol*. 1995;165:1223-1228.
16. Cortes AR, Abdala-Junior R, Weber M, Arita ES, Ackerman JL. Influence of pulse sequence parameters at 1.5 T and 3.0 T on MRI artefacts produced by metal-ceramic restorations. *Dentomaxillofac Radiol*. 2015;44:20150136.
17. Gee CS, Nguyen JT, Marquez CJ, et al. Validation of bone marrow fat quantification in the presence of trabecular bone using MRI. *J Magn Reson Imaging*. 2015;42:539-544.

18. Kullberg J, Ahlstrom H, Johansson L, Frimmel H. Automated and reproducible segmentation of visceral and subcutaneous adipose tissue from abdominal MRI. *Int J Obes (Lond)*. 2007;31:1806-1817.
19. Yeung DK, Griffith JF, Antonio GE, Lee FK, Woo J, Leung PC. Osteoporosis is associated with increased marrow fat content and decreased marrow fat unsaturation: a proton MR spectroscopy study. *J Magn Reson Imaging*. 2005;22:279-285.
20. Blomlie V, Rofstad EK, Skjonsberg A, Tvera K, Lien HH. Female pelvic bone marrow: serial MR imaging before, during, and after radiation therapy. *Radiology*. 1995;194:537-543.
21. Huang W, Yang Y, Sun Z, Zeng X. Early radiation-induced bone marrow injury: serial MR imaging during initial 4 weeks after irradiation. *Acad Radiol*. 2009;16:733-738.
22. Skorpil M, Ryden H, Wejde J, Lidbrink E, Brosjo O, Berglund J. The effect of radiotherapy on fat content and fatty acids in myxoid liposarcomas quantified by MRI. *Magn Reson Imaging*. 2017;43:37-41.
23. Arita ES, Pippa MG, Marcucci M, et al. Assessment of osteoporotic alterations in achondroplastic patients: a case series. *Clin Rheumatol*. 2013;32:399-402.
24. Aguiar MF, Marques AP, Carvalho AC, Cavalcanti MG. Accuracy of magnetic resonance imaging compared with computed tomography for implant planning. *Clin Oral Implants Res*. 2008;19:362-365.
25. Gray CF, Redpath TW, Smith FW, Staff RT. Advanced imaging: magnetic resonance imaging in implant dentistry. *Clin Oral Implants Res*. 2003;14:18-27.
26. Pompa V, Galasso S, Cassetta M, Pompa G, De Angelis F, Di Carlo S. A comparative study of magnetic resonance (MR) and computed tomography (CT) in the pre-implant evaluation. *Ann Stomatol (Roma)*. 2010;1:33-38.
27. Ma J. Dixon techniques for water and fat imaging. *J Magn Reson Imaging*. 2008;28:543-558.

Reprint requests:

Arthur Rodriguez Gonzalez Cortes, DDS, PhD
Department of Oral Radiology
School of Dentistry
University of São Paulo
Av. Lineu Prestes, 2227
Sao Paulo, SP 05508-000
Brazil
arthuro@usp.br